ANTI-TUMOR IMMUNE RESPONSES AGAINST MTLN3 MAMMARY ADENOCARCINOMA

THESIS

Presented to the Graduate Council of the

Graduate School of Biomedical Sciences

University of North Texas

Health Science Center at Fort Worth

in Partial Fulfillment of the Requirements

For the Degree of

MASTER OF SCIENCE

By

KiahRae Carter, B.S.

Fort Worth, Texas

April, 2014

TABLE OF CONTENTS

CHAPTER I

INTRODUCTION AND BACKGROUND

Breast Cancer Pathogenesis

Breast cancer is the most commonly diagnosed cancer in women and is the leading cause of cancer-related mortality (5). The National Cancer Institute at the National Institutes of Health estimates 232,340 new cases will be diagnosed in women and of those 39,620 will die in 2013. Common treatments for breast cancer include, but not limited to, surgery, chemotherapy, and radiotherapy. One of the major side effects that can result from these treatments is secondary lymphedema, an excess of lymph fluid in interstitial space most commonly located in the arm. Other side effects of these treatments can include hair loss, fatigue, anemia, pain, nausea and vomiting, etc. While there is much research investigating therapies for the treatment of breast cancer, there is still a need for research investigating the side effects of breast cancer treatment.

During breast cancer, primary tumors consist of heterogeneous populations of cells with genetic alterations that allow them to surmount physical boundaries, disseminate and colonize a distant organ (24). Metastasis is a succession of these events (24). The first stage in breast cancer metastasis involves the loss of local constraints, both physical and regulatory, emanating from neighboring normal cells and surrounding

stroma (33). Intravasation is the second step and involves the breast tumor cells entering a circulatory system (blood and/or lymphatic) (33). Finally, the tumor cells must disseminate, survive hostile environments and colonize to distant organs (33). Breast cancer cells that have metastasized into the nearby lymph nodes, via the lymphatics, suggest the patient will have an increased risk of the cancer spreading to other organs.

Cells from malignant primary tumors can spread from their sites of origin to invade local tissue and enter the systemic circulation to spread to other organs via the blood vessels and lymphatics (19). Lymphangiogenesis, the growth of new lymphatic vessels, is regulated by the signaling system of vascular endothelial growth factor (VEGF) molecules (VEGF-C, VEGF-D) and its receptor VEGFR-3 (19). Binding of the glycoprotein ligand, VEGF-C/D, to its receptor, VEGFR-3, promotes vascular permeability, angiogenesis, and lymphangiogenesis (19). Lymphatic vessels offer the tumor cells a more advantageous route of invasion and metastasis to other organs through their loose cell-cell junctions, having a lower flow rate that increases survival of cells by minimizing shear stress and having a higher lymph concentration of hyaluronic acid, a molecule with cell protecting and pro-survival qualities (21). While VEGF-C/D is known to be important in breast cancer metastasis, its role in secondary lymphedema is still poorly understood.

The presence of tumor metastases in the axillary lymph nodes of breast cancer patients has been one of the most important prognostic factors for diagnosing breast cancer (14). The sentinel lymph nodes are the first nodes reached by metastasizing cancer cells flowing through the lymph fluid from the tumor site. Sentinel lymph node biopsy has become a common procedure in patients with metastatic breast cancer to stage the cancer (15). Treatment of the axilla in the case of a negative sentinel lymph node biopsy can be safely omitted, whereas, a

positive sentinel lymph node biopsy is indicative of a complete axillary lymph node dissection (15). However, a complete axillary lymph node dissection in breast cancer patients can lead to long-term complications such as pain, nerve injury and/or secondary lymphedema (15).

Immunity to Breast Cancer

The immune system plays a major role in the detection and elimination of cancer cells and nascent tumors through immunosurveillance of cells and tissues in the body (7). The immune system is divided into innate and adaptive immunity with crosstalk between the two (8). Innate immunity is non-specific and is activated within hours of infection, making it the first to respond to foreign antigens. Complement proteins, along with, macrophages (MAC), granulocytes, natural killer cells (NK cells) and dendritic cells (DC) are a few of the key players in the innate immune response (9). Innate immunity exerts its rapid effector function to cancer cells through a limited repertoire of germline-encoded receptors such as pattern recognition receptors (8, 9). Macrophages, activated by interferon-gamma, have high cytotoxicity toward tumor cells by releasing high levels of toxic intermediates such as lysosomal enzymes, nitric oxide , reactive oxygen intermediates, and tumor necrosis factor (10). NK cells are cytolytic effector lymphocytes, which can directly induce the death of tumor cells without prior sensitization (8, 12). NK cells use a combination of inhibitory and activating receptors such as the killer-cell immunoglobulin-like receptors to detect the loss of major histocompatibility complex (MHC) class I expression on cancer cells. NK cells can also express NKG2D receptors which recognize their ligand, MICA or MICB, expressed by cancer cells to induce their killing (9). Dendritic cells play a critical role in bridging innate and adaptive immunity (11). Dendritic cells are professional antigen presenting cells, presenting phagocytosed tumor-cell debris for MHC presentation to stimulate tumor-specific lymphocytes responses in the regional node (9).

The adaptive immune response occurs much later in the disease process (days as opposed to hours), it is antigen specific and can generate memory cells. T and B-cells are the two types of lymphocytes that characterize the adaptive immune response (8). The delayed response is due to the expansion of rare lymphocytes that harbor somatically rearranged immunoglobin molecules such as the B cell receptors or T cell receptors that are specific for microbial derived proteins or processed peptides presented by MHC molecules (9). T cells can be divided into two-subtypes: CD4+ and CD8+ T cells. CD4+ T-cells, also known as helper T-cells (Th1 or Th2), recognize peptides presented by antigen presenting cells through MHC Class II pathway (9). Th1 cells activate CD8+ T cells, through the secretion of interleukin-2 and macrophages through the secretion of interleukin-2, interferon-gamma, and tumor necrosis factor-β to elicit their cytotoxic functions to cancer cells (9). Th2 cells can also further stimulate B cells that have picked up and phagocytosed their antigen, then presented antigen to Th2 cells, through CD40-CD40L interaction and the secretion of interleukin-4, 5, and 6. B cells, in turn, become effector plasma cells and can produce antibodies specific for tumor antigens. These antibodies to cancer cell-surface molecules can inhibit oncogenic signaling (9).

NK cells can recognize the Fc region on antibodies, which have coated tumor cells, through their Fc receptor and can kill the tumor cells directly via antibody dependent cell-mediated cytotoxicity (13). CD8+ T cells, also known as cytotoxic T cells recognize peptides presented by MHC Class I pathway (9). They kill tumor-cells through the Perforin-Granzyme pathway and death ligands, such as FAS and tumor-necrosis factor (9). They also secrete interferon-gamma to inhibit tumor growth.

Though most activated B cells and T cells become short-lived effector cells, some become memory effector cells. Memory B cells and T cells are generated after the first immune

response (primary response) to a tumor antigen. These memory cells can be central memory cells, reside in lymphoid tissue, or effector memory cells, reside in tissue where antigen was picked up (13). When they encounter antigen for the second time, their response is much quicker than the primary response. The innate and adaptive immune systems, together, play a crucial role in detecting cancer cells early (innate) and controlling breast cancer long term (adaptive).

The immune system can be further divided into mucosal immunity, which includes gut-associated lymphoid tissues (GALT) and bronchial-associated lymphoid tissues (BALT). Mucosal surfaces are the main port of entry for antigens, especially in the gut. GALT is comprised of peyer's patches, appendix and lymphoid nodules (44). It also consists of effector B cells, T cells and phagocytes that can sample luminal antigens through the follicular associated epithelium (45). This sampling is important for the differentiation of beneficial or harmful antigens (from food) or microbes in the gut lumen (45). The follicular associated epithelium contains M cells, which can transport antigen from gut lumen via transcytosis into the basal cell membrane (44). Here, dendritic cells can pick up antigen and present to T cells to become effector cells (44). These activated lymphocytes can traffic via the lymphatic's that drain the intestines and travel to the thoracic duct (44). Once in the thoracic duct they can circulate the entire body, going back into mucosal tissue such as the BALT and GALT via small blood vessels that line MALT, which express mucosal adressin MAdCAM-1 (44). However, the role of the mucosal immune system in cancer immunity still needs further investigation.

The Lymphatic System and Lymphedema

The lymphatic system can play a significant role in the pathogenesis of breast cancer. The lymphatic system is an organized network, composed of functionally interrelated tissue and transportation pathways of lymph fluid and lymphoid cells (22). Its main components are

immune cells, organized lymphoid tissue such as thymus, spleen, lymph nodes, bone marrow, and lymphoid tissue in gut and lungs (22). It also contains vessels and fluids such as tissue fluid and lymph (22). The flow of lymph fluid through the lymphatic vessels is unidirectional, mediated by the contraction of the vessel walls and valves that prevent fluid from going backwards. One of the main functions of the lymph system is to transport antigens from tissues to lymphoid organs to be able to induce an immune response against foreign antigens while maintaining tolerance to self-antigens (22). It also functions to maintain tissue fluid homeostasis (22). Disease processes, such as breast cancer and its treatment, that impede lymph flow can lead to lymphedema (16).

Secondary arm lymphedema is a chronic and distressing condition that can affect women undergoing treatment for breast cancer or can occur years after their treatment (18, 22). The lymphatic system functions to return excessive interstitial fluid to the blood circulation, while allowing leukocytes to sample the internal environment for foreign antigens. (16). When this process is impaired, as is the case of breast cancer patients undergoing complete axillary lymph node dissection, secondary arm lymphedema can occur (16, 17). Lymphedema results in excess fluid accumulation in the interstitial space (18). Patients who develop lymphedema are predisposed to the development of other secondary complications, such as infections of the upper limb, psychological sequelae, the development of malignant tumors and alterations to their quality of life (17). There is no cure for secondary lymphedema and its side effects are irreversible. Therefore, there is a need to study therapies to treat the damaging side effects of secondary lymphedema.

Physical Medicine Therapies for the Treatment of Secondary Lymphedema

As lymphedema generally worsens over time, health professionals have sought therapies

to decrease limb swelling and other associated problems that develop from edema (18). Several methods have been developed and reviewed for the treatment of secondary arm lymphedema. Outside the United States, lymphedema has been treated with coumarin, which may help edema by reducing vascular permeability, protein, and extracellular fluid accumulation. It's also thought to stimulate lymph flow and reduce protein concentration and fibrotic induration in the tissues by stimulating proteolysis (17, 18). However, the Mayo Clinic investigated this drug further in a randomized study and they concluded that coumarin was an ineffective therapy for women who developed arm lymphedema after breast cancer treatment (17). This finding could suggest that LET may be better for treating secondary lymphedema.

Manual lymphatic drainage uses various light massage techniques to help remove excess interstitial fluid, increase lymphatic transport and soften fibrotic induration (18). Decongestive lymph treatment combines manual lymph drainage, compression bandages and pneumatic pumps. Pneumatic pumps can be used to encourage fluid drainage from the distal to the proximal end of the limb. It works by using a single or multiple chambered pump that envelops the limb and inflates and deflates at different cycles and pressures (18). Takeno et al, found that the application of complete decongestive therapy to an edematous rat limb encouraged lymph fluid to move from the periphery (43). Compression bandaging helps decrease the amount of interstitial fluid formation, prevents the back flow of lymph and enhances the muscle pump by providing an inelastic barrier for the muscle to work against (18). Complex physical therapy is another treatment used. It involves two to four weeks of manual lymphatic drainage followed by compression bandaging and skincare plus prescribed limb exercises. The patient is then fitted with a compression garment, which helps to decrease the amount of interstitial fluid formation and prevent lymph back flow (18).

Exercise is another common therapy for secondary lymphedema and is often used in conjunction with manual lymph drainage, decongestive lymph therapy and complex physical therapy. Physical exercise has the ability to stimulate innate immune responses and control angiogenesis (6). Friedenreich et al, found with physical exercise there was a risk reduction between 10-30% of developing breast cancer (6). One study found that patients involved in exercise after chemotherapy or radiation, compared with those patients who did not exercise after treatment, had an increase in lymphocyte activation (31). Physicians and physiotherapists have feared for a long time exercise would exacerbate lymphedema, therefore, having their patients perform minimal exercise routines. Author of the Physical Activity and Lymphedema trial found there was no increase incident of lymphedema with a slow-progressive weight-lifting exercise regimen (6). Another study found high intensity exercise lead to an increase in life-span, decrease in tumor mass and prevented indicators of cachexia in rats with tumors (25). However, more studies still need to be investigated on exercise and lymphedema, with programs being individualized to each patient.

Osteopathic physicians believe removing obstructions to tissue, blood, and lymph flow, as resulting from edema, is one of the most effective ways to promote and restore health (23). They utilize lymphatic pump treatment (LPT) to improve lymphatic flow, enhance immunity and treat infections and lymphedema (23, 34). Many clinical benefits of LPT have been reported, the mechanism of how it provides protection and enhances immunity are not clearly understood. Studies have found LPT to increase lymph flow and leukocytes in the thoracic and mesenteric duct lymph in dogs and rats (20, 23, 26). Another study has shown after the administration of LPT, there was an increase in flux of inflammatory mediators, such as chemokines, cytokines, reactive oxygen species, and reactive nitrogen species, from the tissue into the lymph (27). These

results support LPT for enhancing lymph flow and releasing immune cells into circulation. However, its use as a complementary and alternative medicine therapy still needs further investigation.

While lymph enhancing therapies relieve the symptoms of secondary arm lymphedema, many manual medicine therapists are hesitant to perform these techniques on patients with cancer for the fear of promoting metastasis through the lymphatic system. Currently, there is no scientific proof that lymph enhancing therapies promote metastasis. The MTLn3 mammary adenocarcinoma rat model will closely mimic human breast cancer disease to allow for the study of lymph enhancing therapies and their role on breast cancer metastasis. Our long term goal is to determine if LPT reduces limb edema, enhances immune surveillance and prevents tumor growth and metastasis. In this study, we hypothesized the administration of LPT would enhance immunity and inhibit primary breast tumor growth

CHAPTER II

THE ROLE OF LPT IN F344 RATS WITH MTLN3 MAMMARY ADENOCARCINOMA

Introduction

The purpose of the present study was to investigate the role of LPT on breast cancer metastasis. To do this, we used the MTLn3 mammary adenocarcinoma tumor cell line which mimics human breast cancer (3). This model forms primary breast tumors and is highly metastatic, metastasizing to the axillary lymph nodes and lungs around three weeks after injection (1, 2, 3). However, little is known about the immune response to MTLn3 during its disease timeline of twenty-five days. The first objective of this study was to characterize the immunologic response to MTLn3 mammary adenocarcinoma and determine if LPT augments this response. Based on previous reports (1, 2, 3), we predicted that leukocyte populations would increase in the lymph nodes, spleen and lung between days fourteen to twenty-five. Secondly, we hypothesized the administration of LPT would enhance immunity and inhibit primary breast tumor growth. However, further studies will be needed to confirm if LPT is safe and if it will reduce edema in patients with secondary arm lymphedema.

Materials and Methods

Animals. Immune competent female inbred Fischer 344 (F344) rats (Harlan Laboratories, Houston, TX) weighing between 150-174 grams were used in these studies. Rats were housed and fed according to the Institutional Animal Care and Utilization Committee (IACUC) of the University of North Texas Health Science Center in the barrier facility. Rats' body weight were monitored weekly throughout twenty-five days.

Tumor Cell Culture and Inoculation. MTLn3 is a highly metastatic mammary adenocarcinoma cell line that mimics human breast cancer and was originally obtained from a pulmonary metastasis of a F344 rat, named 13762NF (1, 2, 3). The MTLn3 cell line (Provided by Jeffrey Segall, Albert Einstein College of Medicine of Yeshiva University) was maintained in a monolayer cell culture at 37°C and 5% CO_2 with minimum essential medium (MEM) (Invitrogen, Carlsbad, CA) with 5% fetal bovine serum (FBS) (Sigma-Aldrich, St. Louis, MO). Cells were harvested from culture flasks by using sterile phosphate buffered saline (PBS) (HyClone, Logan, UT) and trypsin (HyClone) to remove the adherent cells from the surface of the flask. Tumor cells were washed twice and suspended in sterile PBS for cell count using the hemacytometer prior to being injected into the animals. Tumor cell viability was determined by Trypan blue (Sigma-Aldrich) staining. On day zero, rats were anesthetized with ketamine (Miller Vet. Supply, Fort Worth, Texas) and xylazine (Miller Vet. Supply). Rats were then injected sub-cutaneous (sub-Q) with 0.5 mL of $1x10^6$ MTLn3 tumor cells (some injections were with transfected cells) in sterile PBS in the second right mammary fat pad. Rats were humanely euthanized with ketamine (100 mg/kg) and xylazine (15 mg/kg) 0, 7, 14, 21, 25 and 30 days after injection. Primary tumor volume was calculated *in situ* with calipers using the formula: (length x

width$^{2)}$ x (π/6) (4). Data were expressed in cm^3. Primary tumors were then excised and weighed *ex vivo*. Tumor weight data were expressed in grams.

Transfection of MTLn3 Tumor Cells. MTLn3 cells were stably transfected with pZsGreen1-N1 vector (Clontech, Mountain View, CA) using the Xfect Transfection Reagent (containing Xfect Reaction buffer and Xfect polymer) (Clontech). MTLn3 cells were grown to a concentration of 0.125 x 10^6 cells/mL of MEM without antibiotics on a six-well plate. Cells were incubated at 37°C and 5% CO_2 with 5 µg plasmid DNA, 1.5 µL of Xfect Polymer and 88.5 µL Xfect Reaction Buffer for 4 hours to allow for transfection to occur. Transfection media was taken off cells and replaced with 2 mL of fresh MEM medium with no antibiotic and incubated for 48 hours at 37° C and 5% CO_2. Lastly, 400 µg/mL of G418 antibiotic (Clontech) was added to the media to select for transfected cells and incubated for 3-5 days at 37°C and 5% CO_2. Fluorescence was measured using the Olympus IX70 Fluorescence Microscope (Olympus Imaging America Inc., Center Valley, PA).

Treatment Groups. Rats were divided into one of four treatment groups. Treatment groups consisted of control (healthy), MTLn3, MTLn3+Sham-LPT, and MTLn3+LPT animals. Healthy animals received no MTLn3 tumor injection or anesthesia throughout the twenty-five day timeline. Fourteen days post-injection of 1x10^6 MTLn3 tumor cells, MTLn3 group received no treatment or anesthesia, the MTLn3+Sham-LPT group received a daily sham treatment consisting of inhalational administration of isoflurane (Abbott Animal Health, Abbott Park, IL) anesthesia followed by five minutes of light touch for nine days, and the MTLn3+LPT group received five minutes of the following treatments daily under isoflurane anesthesia for nine days:

one minute of diaphragm doming, two minutes of abdominal LPT (Ab-LPT) and two minutes of thoracic LPT (Th-LPT). Rats received 5% inhalational isoflurane anesthesia prior to treatment and remained anesthetized at 2% isoflurane during treatment. Diaphragm doming was performed with the rat supine and pressure was applied to the thoracic cage and diaphragm area to stretch the restricted tissue. To perform Ab-LPT, the operator contacted the rat with the thumb and fingers placed bilaterally at the costal-diaphragmatic junction. Sufficient pressure was exerted medially and cranially to compress the lower ribs until significant resistance was met against the diaphragm, then the pressure was released. Compressions were administered at approximately one per second for the duration of the two-minute Ab-LPT treatment. To perform Th-LPT, the operator's index fingers contacted the lateral aspect of the lower ribs, and bilateral finger pressure was applied for approximately one per second for twenty seconds. This pressure was released for ten seconds to allow for inspiration. This cycle was repeated over two-minutes. On day twenty-five post-injection, rats were euthanized and tissues were collected (Figure 4).

Histology. Lungs, tumor-adjacent lymph nodes (ALN), and tumor-opposite lymph nodes (OLN) were excised at day twenty-five and thirty and fixed in 4% neutral buffered formalin (Fisher Scientific, Pittsburgh, PA) for 48 hours. After fixation, tissues were rinsed in 30% sucrose for one hour, changing solution after thirty minutes. Next, tissues were placed in labeled molds and embedded in optimal cutting temperature (OCT) compound (Sakura Finetek, Torrance, CA) containing 10.24% polyvinyl alcohol, 4.26% polyethylene glycol and 85.5% non-reactive ingredients at room temperature for one hour. Blocks were submerged and frozen with liquid nitrogen. Blocks were wrapped in aluminum foil and were stored at -80°C until ready for sectioning.

To section tissues, blocks were placed in the leica 2800N frigocut cryostat (LEICA Microsystems, Buffalo Grove, IL) for thirty minutes to allow the block to equilibrate to the temperature of the cryostat chamber (14-19°C). The block was then placed on microtome specimen disk and adjusted to appropriate position to begin sectioning. All tissues were cut at 10 µm and were placed on superfrost/plus microscope slides (Fisher Scientific). The slides were dried for two hours at room temperature and then either placed in -80°C for storage or stained.

Tissues were submerged into fixative for 2-5 minutes. Next, they were placed in 70% ethyl alcohol (EtOH) for thirty seconds, and then transferred in 50% EtOH to the sink to wash with deionized (D.I.) water for 2-4 minutes. The slides were placed in hemotoxylin for fifty seconds, were washed with D.I. water for five minutes and were transferred into eosin for thirty seconds. The slides were dipped three-times in 70%EtOH, 95% EtOH and placed in 100% EtOH for five minutes (repeating three times). Slides were placed in 1:1 mixture of 100% EtOH and Xylene for five minutes. Lastly, they were transferred to 100% xylene for five minutes (repeating twice). Coverslips were then placed on the slide with mounting medium and analyzed using the Olympus TIRF microscope (Olympus Imaging America Inc., Center Valley, PA)

Lymphocyte Isolation. Lungs, ALN, OLN and spleens were removed from all groups 0, 7, 14, 21 and/or 25 days post-injection. To prepare lung single-cell suspensions, lungs were placed in RPMI (Hyclone) wash media supplemented with 5% FBS, 1X antibiotics/antimycotics (Hyclone), and 10 mM Hepes (Hyclone). Lungs were finely minced for subsequent tissue dissociation using a gentleMACS dissociator (MACS Miltenyi Biotec, Auburn, CA). Lung cell suspensions were then passed through a nylon mesh filter to remove any non-dissociated tissue. After lung cell suspensions were washed twice with RPMI wash media, they were layered over a

Lympholyte Rat gradient (Cedarlane Laboratories Limited, Burlington, NC) to purify lymphocytes by density gradient centrifugation. Samples were centrifuged at 1200g for 20 minutes, 25^0C, slow break. The lymphocytes separated on the gradient were collected for enumeration using a Hemavet 950 Cell Analyzer (Drew Scientific, Waterbury, CT). The lung lymphocytes were used for flow cytometry.

Single-cell suspensions of ALN and OLN were prepared by passing lymph nodes through a nylon mesh filter. Cells were then washed once in RPMI wash media and red blood cells were removed using ACK lysis buffer (0.15M NH_4Cl, 10mM $KHCO_3$, 0.1mM Na_2EDTA). Cells were collected and washed once more in RPMI wash media, then counted and resuspended in culture media. and OLN lymphocytes were used for Hemavet total cell count and flow cytometry.

Single cell suspensions of spleen cells were prepared by passing spleens through a nylon mesh filter. Cells were then washed twice in RPMI wash media and red blood cells were removed using ACK lysis buffer. Cells were collected and washed 2 more times in RPMI wash media, then counted and resuspended in culture media. The spleen lymphocytes were used for Hemavet total cell count and flow cytometry

Flow cytometry. Immunofluorescent staining of lung, ALN, OLN and spleen lymphocytes was performed using the following monoclonal antibodies: anti-rat-CD3 (T cell) (Biolegend, San Diego, CA), -CD4 (T cell) (Biolegend), -CD8 (T cell) (Biolegend), -CD161 (NK cell) (Biolegend), -CD45RA (B cell) (Biolegend), -CD11c (Dendritic cell) (BioRad, Hercules, CA), – Macrophage (BD Bioscience, San Jose, CA) and -IFN-γ (Biolegend) was used for intracellular cytokine staining. Lung, ALN, OLN or spleen cells were plated at 1 x 10^6/100µL in a 96-well plate and incubated with 50µL of phorbol 12-myristate 13 acetate (PMA) /Ionomycin (Sigma)

solution for 1 hour at 37° C and 5% CO_2. Additionally, 15µL of Brefeldin A (BFA) (Biolegend) was added to each well and incubated for 3-4 hours at 37° C and 5% CO_2. After incubating, the plates were centrifuged at 1500 RPM for 5 minutes at 4°C. Following removal of supernatant, lung, ALN, OLN and spleen cells were fixed with 100µL of fixation buffer (Biolegend) and stored at 4°C overnight. The next day, cells were washed with 200 µL of 1X permeabilization buffer (Biolegend) and incubated with the optimal concentration of monoclonal antibody for 30 minutes in the dark at room temperature. Separate 100µL aliquots of each tissue cell sample were single stained with 2.25µL of CD3, 5.625 µL of CD4, 22.5µL of CD8, 4.5µL of CD161 and 90µL of IFN-γ. After incubating with fluorescent stains, cells were again washed with 200 µL of permeabilization buffer and washed twice with 200 µL of staining buffer. One 100µL lung, ALN, OLN and spleen aliquot was left unstained to serve as a negative control. Lastly, cells were brought up to 500 µL of staining buffer. Cells were subjected to the BD LSR II flow cytometer (BD Bioscience, San Jose CA) and data was analyzed using FlowJO software (TreeStar Inc., Ashland, OR). Cell populations were detected from histogram peaks or dot plot cell clusters. Each cell population was expressed as the percentage of the number of stained cells. To calculate the total number of a specific lymphocyte population, their percentage was multiplied by the total number of cells in lung, ALN, OLN or spleen samples as determined by the Hemavet count.

Leukocyte Counts. Blood, lung, ALN, OLN, and spleen samples were analyzed for leukocyte numbers. To prepare lung, ALN, OLN and spleen tissue samples for leukocyte enumeration, tissue samples were treated as described in the previous section. Cardiac blood samples were collected 0, 7, 14, 21 and 25 post-injection of tumor cells. Total leukocyte and differential

leukocyte counts for each blood, lung, ALN, OLN and spleen sample were determined by the Hemavet.

Statistical analysis. Data from control, MTLn3, MTLn3+Sham-LPT and MTLn3+LPT were analyzed using GraphPad Prism version 5.0 for Mac OS X (GraphPad Software, San Diego, CA). Statistical analysis was retrieved using analysis of variance (ANOVA) with Kruskall-Wallis or Tukey post-test. Correlation analysis between tumor size and total leukocytes in the spleen was performed using spearman coefficient. Differences among mean values with $P \leq 0.05$ were considered statistically significant. Data are expressed as mean ± SEM.

Results

Primary tumor growth increased during disease

Primary breast tumor size is an indicator of disease staging and pathogenesis (36). Consistent with previous studies, MTLn3 primary tumors were not palpable until day fourteen post-injection (1). Between days 14-25, there was a gradual increase in tumor size (Figure 1). There was a ninety-three fold increase in tumor weight. Tumor weight (Figure 1a), measured *ex vivo*, increased from 0.058 ± 0.006 grams on day fourteen to 5.404 ± 1.051 grams on day thirty. There was a 188-fold increase in tumor volume. Tumor volume (Figure 1b) was measured *in situ* and increased from 0.027 ± 0.005 cm^3 on day fourteen to 5.065 ± 0.34 cm^3 on day thirty. This data suggests significant primary tumor growth between days 14-30.

MTLn3 induced pathology in the tumor-adjacent lymph node

Sentinel lymph nodes are the first nodes metastasizing cancer cells reach when metastasizing through the lymph from the primary tumor site. To determine if MTLn3 induced

pathology in the tumor-adjacent lymph nodes and tumor-opposite lymph nodes compared to control, ALN and OLN were excised at days twenty-five and thirty post-injection. Tissues were sectioned and stained with hematoxylin and eosin (H&E). Our preliminary results confirmed that MTLn3 induced pathology in the tumor-adjacent lymph node when compared to the tumor-opposite lymph node on day twenty-five (Figure 2a). This pathology was confirmed with H&E staining, comparing control and MTLn3 tumor-adjacent lymph nodes at day thirty (Figure 2b). These results are consistent with previous reports of MTLn3 metastasizing to the axillary lymph nodes (1). In future studies, we will quantify MTLn3 disease using histopathological scoring.

Splenic leukocytes expanded by day twenty-five

Innate and adaptive immunity plays a very important role in the detection and eradication of cancer cells and tumors through immune surveillance of cells and tissues (7). To determine if there was an increase in leukocytes in the spleen, rats were subcutaneously injected with tumor cells. On days 0, 7, 14, 21 and 25 post-injection, splenic leukocyte populations were quantified by flow cytometry. As seen in the spleen between days 14-21, there was an increase in all cell populations (Table 1). Specifically, the B cells increased sixteen-fold from day zero to day twenty-one (3.27 ± 0.32 to 51.2 ± 12.6). CD4+ T cells were also increased seven-fold by day twenty-one (14.1 ± 2.90 to 97.6 ± 36.3). By day twenty-one, CD8+ T cells, NK cells, DCs and MACs increased 1.5-3.25 fold. Between days 21-25, CD4+ T cells decreased seven-fold (97.6 ± 36.3 to 14.5 ± 1.31). B cells decreased three-fold between days 21-25 (51.2 ± 12.6 to 15.3 ± 1.60). CD8+ T cells, DCs, NKs and MACs decreased 1-3 fold by day twenty-five. This suggests that by day twenty-one of disease, splenic leukocytes have expanded. The decrease measured at day twenty-five is likely due to leukocytes trafficking to diseased tissues such as the tumor-adjacent lymph node and/or primary tumor.

Splenic leukocyte concentrations do not correlate with tumor size

An unexpected finding in this study was the decrease in leukocytes between days twenty-one to twenty-five. To determine if tumor size was associated with leukocytes in the spleen, comparisons were made between total splenic leukocytes and tumor size on days twenty-one and twenty-five. On day twenty-one, tumor size was between 0.5-1.5 grams and there were $1.61 \times 10^8 \pm 2.66 \times 10^7$ total leukocytes in the spleen (Figure 3a). By day twenty-five, total leukocytes decreased to $9.11 \times 10^7 \pm 5.24 \times 10^6$ and average tumor size was greater that two grams (Figure 3b). A correlation analysis showed there was no significant correlation between tumor size and total leukocytes in the spleen. This data would suggest that splenic leukocytes are not mediated by the size of the tumor. Further, this data could provide more support that leukocytes are trafficking from the spleen to diseased sites such as tumor-adjacent lymph nodes and primary breast tumor.

Leukocytes increased in the tumor-adjacent lymph node

The presence of tumor cells in the tumor-adjacent lymph node could promote leukocyte entry into the lymph nodes. MTLn3 metastasized to the ALN by day twenty-five post-injection (1). Therefore, to determine if there was an increase in leukocytes in tumor-adjacent lymph node in response to disease, ALN and OLN leukocyte populations were quantified 0, 7, 14, 21 and 25 days post-injection. At day twenty-five in the tumor-adjacent lymph nodes, all leukocyte populations increased significantly ($p < 0.05$) compared to day zero (Table 2a). The most impressive increase was seen in macrophages, which increased thirty-seven fold between days zero (0.55 ± 0.11) and twenty-five (20.1 ± 6.07). B cells and natural killer cells also increased ten-fold between days 0-25. In the tumor-opposite lymph node, there were no significant increase in any leukocyte population with the exception of natural killer cells, which increased

4.5-fold by day twenty-five when compared to day zero (0.14 ± 0.04 to 0.63 ± 0.18) (Table 2b). The NK cells may be surveying the OLN for tumor cells. This data suggests that sentinel node metastasis promotes leukocyte, specifically macrophages, entry into the tumor-adjacent lymph node.

Leukocytes migrated into lung between days fourteen to twenty-five

Previous studies reported lung metastasis by day twenty-five (1, 2, 3). To determine if leukocytes trafficked into the lung due to the presence of tumor cells, pulmonary leukocyte populations were quantified using flow cytometry. Pulmonary leukocytes remained relatively unchanged during the twenty-five days of disease with the exception of natural killer cells, dendritic cells and B cells (Table 3). Dendritic cells increased two-fold at day fourteen when compared to day zero (0.31 ± 0.08 to 0.59 ± 0.08), suggesting that tumor cells may have been present in the lung. Interestingly, B cells decreased 2.5-fold by day twenty-five when compared to day zero (2.62 ± 0.46 to 1.03 ± 0.31), suggesting they may have migrated to the regional lymph nodes to be further activated. Natural killer cells were increased seven-fold on day twenty-one when compared to day zero (0.16 ± 0.04 to 1.15 ± 0.31). It's likely that NK cells have trafficked in due to tumor cells seeding in the lung.

LPT did not enhance tumor growth

Currently, it is not known whether LPT enhances tumor growth and metastasis. Therefore, to determine if LPT enhanced MTLn3 primary tumor growth, rats were subcutaneously injected with MTLn3 tumor cells and received sham treatment or LPT for nine days as described in Figure 4. On day twenty-five, primary tumors were measured *in situ* to determine tumor volume and were then weighed *ex vivo*. There were no significant changes in

tumor volume and weight between MTLn3, MTLn3+Sham-LPT and MTLn3+LPT groups (Figure 5), suggesting sham treatment and LPT does not enhance tumor growth.

Sham and LPT cause weight loss

To determine if LPT treatment has any effect on body weight, rats were subcutaneously injected with MTLn3 tumor cells and divided into MTLn3, MTLn3+Sham-LPT or MTLn3+LPT group for nine days as previously described (Figure 4). Body weights were measured weekly throughout the twenty-five days of disease. Both, Sham-LPT and LPT rats failed to gain weight at days 14-25 of the study compared to rats in the MTLn3 group (Figure 6). This outcome was likely due to the daily administration of anesthesia in both the Sham-LPT and LPT groups. In support, during previous studies using healthy rats, the Sham-LPT and LPT groups also failed to gain weight. Collectively, this data suggests the administration of anesthesia during LPT and sham treatment induces weight loss. However, the effect of this weight loss on cancer growth and metastasis is still unknown.

LPT protects against the pathogenesis induced by anesthesia in the tumor-adjacent lymph node

Anesthesia decreased body weight and, therefore, may have additional clinical and/or pathological outcomes. A previous study found lymph node weight increased significantly after tumor inoculation, suggesting enlargement could be due to hyperplasia of lymph node cells or growth of tumor cells (28). To determine if LPT changed tissue weights, animals were divided into control group or were subcutaneously injected with MTLn3 tumor cells and placed into MTLn3, MTLn3+Sham-LPT or MTLn3+LPT group. On day twenty-five, ALN, OLN, lungs and spleens were excised and weighed (Figure 7). In the tumor-opposite lymph nodes, lungs and spleens, there were no significant changes in tissue weights between groups. However, in the tumor-adjacent lymph node there was a significant increase ($p < 0.05$) in weight in the

MTLn3+Sham-LPT group when compared to control rats. Of interest, the tumor-adjacent lymph node weights following LPT was similar to MTLn3 group. This data suggests, LPT negates the effect of sham-LPT in the lymph node, as seen in the MTLn3+Sham-LPT group.

Sham and LPT inhibit leukocytosis during MTLn3 disease

To determine if the presence of a primary tumor increased the numbers of leukocytes in the blood, rats were divided into control group or were subcutaneously injected with MTLn3 tumor cells and placed into MTLn3, MTLn3+Sham-LPT or MTLn3+LPT group for nine days as previously described (Figure 2). On day twenty-five, cardiac blood was taken and total and differential leukocyte counts were quantified using a Hemavet 950 cell analyzer. All leukocyte populations were significantly increased ($p < 0.05$) for animals in MTLn3 group when compared to all other groups (Table 4). There were no significant changes in any leukocyte population among control, MTLn3+Sham-LPT or MTLn3+LPT group. This data suggests the presence of MTLn3 disease alone promotes leukocytosis. However, when sham and LPT are applied, this effect is negated. This is likely due to the immune suppressing effects documented with isoflurane (37).

Sham and LPT induce pathology in the lung during MTLn3 disease.

To determine if MTLn3 induced pathology in the lung, rats were divided into control group or were subcutaneously injected with MTLn3 and placed into MTLn3, MTLN3+Sham-LPT or MTLn3-LPT group for nine days as previously described (Figure 4). The presence of MTLn3, alone, induced pathology when compared to control group (Figure 8). However, in both the sham-LPT and LPT groups, there was increased pathology compared to just disease alone. This effect was likely due to the administration of isoflurane on days 14-24 of the study. Future studies will include control, sham-LPT and LPT groups without the injection of MTLn3 to

determine if isoflurane alone induced this pathology. Also, we will compare MTLn3+Sham-LPT and MTLn3+LPT groups to determine if LPT alone exacerbates disease in the lungs.

Discussion

Many manual medicine therapists are reluctant to perform lymph enhancing therapies in patients with cancer for the fear of promoting tumor growth and metastasis (30); however, there is no scientific proof to support this hypothesis. In this study, we found LPT did not increase primary tumor size. This result suggests that LPT does not promote primary tumor growth in the mammary tissue. However, more experimentation is necessary to determine if LPT is safe in patients with primary breast tumors.

Previously, we reported that LPT inhibits pulmonary tumor development (39) and reduced bacterial load during pneumonia (40, 41) in a rat model. In addition, LPT has been used clinically to protect against pneumonia (35, 42). Collectively, these studies suggest LPT protects against pulmonary disease. LPT may offer protection due to the redistribution of immune cells from the GALT to the lung. This could be due to the constant sampling of antigens that is taking place in the gut, causing leukocytes to be in an activated state. When LPT is applied, these leukocytes are mobilized into lymph, as found by Hodge et. al. (23), and could home into lung mucosal tissue via MAdCAM-1. However, it is unknown if LPT protects against disease outside of the lung. Using the rat mammary adenocarcinoma cell line MTLn3, we investigated the effects of LPT on primary breast tumor growth, the draining lymph nodes and clinical signs of disease. We found LPT did not enhance primary breast tumor growth nor did it enhance clinical signs of disease. In addition, LPT reduced signs of pathology in the tumor-adjacent lymph node compared to Sham-LPT. Collectively, this data suggests LPT does not alter primary breast

tumor size but may offer protection against disease in the draining lymph node. This mechanism responsible for this result is still under investigation.

At day twenty-five post-injection, the tumor adjacent lymph nodes were enlarged in all groups. Of interest, MTLn3+Sham-LPT significantly ($p < 0.05$) increased the size of the lymph node compared to MTLn3 and MTLn3+LPT groups, suggesting Sham-LPT may be pathologic during the progression of MTLn3 disease. It is likely that the daily administration of anesthesia during Sham-LPT is promoting metastasis in the adjacent lymph node. In support, anesthetics have been documented to cause immune suppression and promote metastasis during cancer (37). This theory is supported by the decrease of blood leukocytes in Sham-LPT and LPT groups. Of interest, lymph nodes in the MTLn3 and LPT groups were similar, suggesting LPT negated the pathology induced during Sham-LPT. It is important to note that we have not identified whether MTLn3 cells have metastasized into the adjacent lymph node and whether LPT protects against sentinel node metastasis.

By day twenty-one, all leukocytes had expanded in the spleen. The results from this study suggest tumor cells and/or antigen have drained into the spleen by day twenty-one, been picked up by B cells and proliferated to become effector cells. Macrophages and dendritic cells may have also picked tumor antigen up in the periphery, trafficked into the spleen, presented to T cells and B cells, which lead to their proliferation and increase in their cell numbers. After expanding, some of these cells may have left the spleen and travelled to diseased sites such as the primary tumor and tumor-adjacent lymph nodes, where there was a significant increase in all leukocyte populations by day twenty-five. Whether LPT augments leukocyte populations in the spleen is currently under our investigation.

With the exception of NK cells, DCs and B cells, all other pulmonary leukocyte populations remained unchanged during disease. Natural killer cells are innate immune cells that function as cytolytic effector lymphocytes that can directly induce killing of tumor cells without prior sensitization (8, 12). In the lung, they increased seven-fold between days 0-21 and they may be initiating anti-tumor responses. Lymphocytes did not increase during the twenty-five days of disease suggesting adaptive immunity is not playing a significant role at this time. However, B cells decreased at day twenty-five, which suggests they have phagocytosed their specific tumor-antigen and migrated to the regional lymph nodes to be further activated. Future studies will measure immune responses at later time points to identify the role of T cells and B cells during MTLn3 disease. In addition, regional lymph nodes will be examined for T cell and B cell activities.

While our current study demonstrates LPT does not enhance primary tumor size, its effect on metastasis is still unknown. In future studies, we will identify whether LPT protects against sentinel node and systemic metastasis. In these experiments, the presence of MTLn3 in the lymph node and lung tissue will be determined by histological analysis. Microvessel density is a quantitative measure of angiogenesis and risk of metastasis (38). To determine if LPT enhances microvessel density, both endothelial and lymphatic microvessel density will be determined by immunohistochemistry.

In conclusion, our data suggests that LPT does not alter (influence or inhibit) primary breast tumor growth. Nevertheless, our data suggests LPT may also protect from the pathogenesis exhibited by MTLn3+Sham-LPT group for tissue weights. One limitation to this approach is the use of isoflurane during sham-LPT and LPT. Further studies are required to

determine if LPT exacerbates disease when compared to sham treatment. In future studies we will confirm if LPT is safe and will reduce edema in patients with secondary arm lymphedema.

CHAPTER III

ILLUSTRATIONS

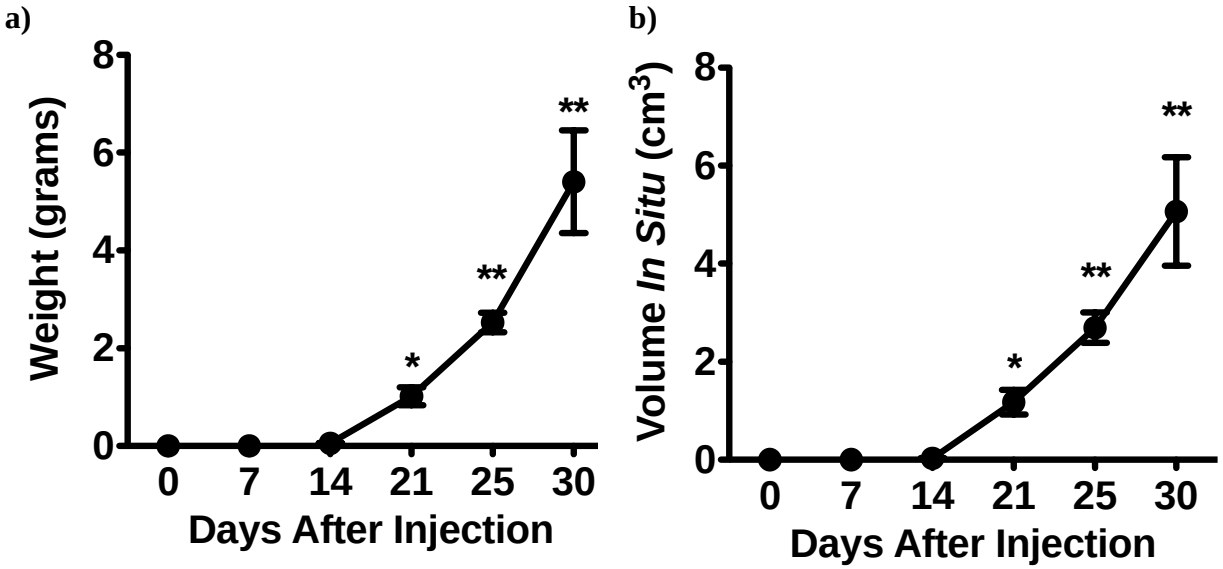

Figure 1. Primary tumor growth increased during disease. On day 0, rats were subcutaneously injected with $1x10^6$ MTLn3 cells/mL. On days 0, 7, 14, 21, 25 or 30 post-injection, rats were euthanized and primary tumors were collected. Tumor weights were measured *ex vivo.* Tumor volume was measured *in situ* with calipers and calculated volume using the equation: $(L \times W^2) \times (\pi/6)$. Data are means ± SEM weight in grams (left) and volume in cm^3 (right) for 5 experiments. Statistical analysis was performed using One-Way ANOVA with Kruskal-Wallis post-test. * denotes $p < 0.001$, and ** denotes $p < 0.0001$ when compared to day 0. N=5-10 rats per group.

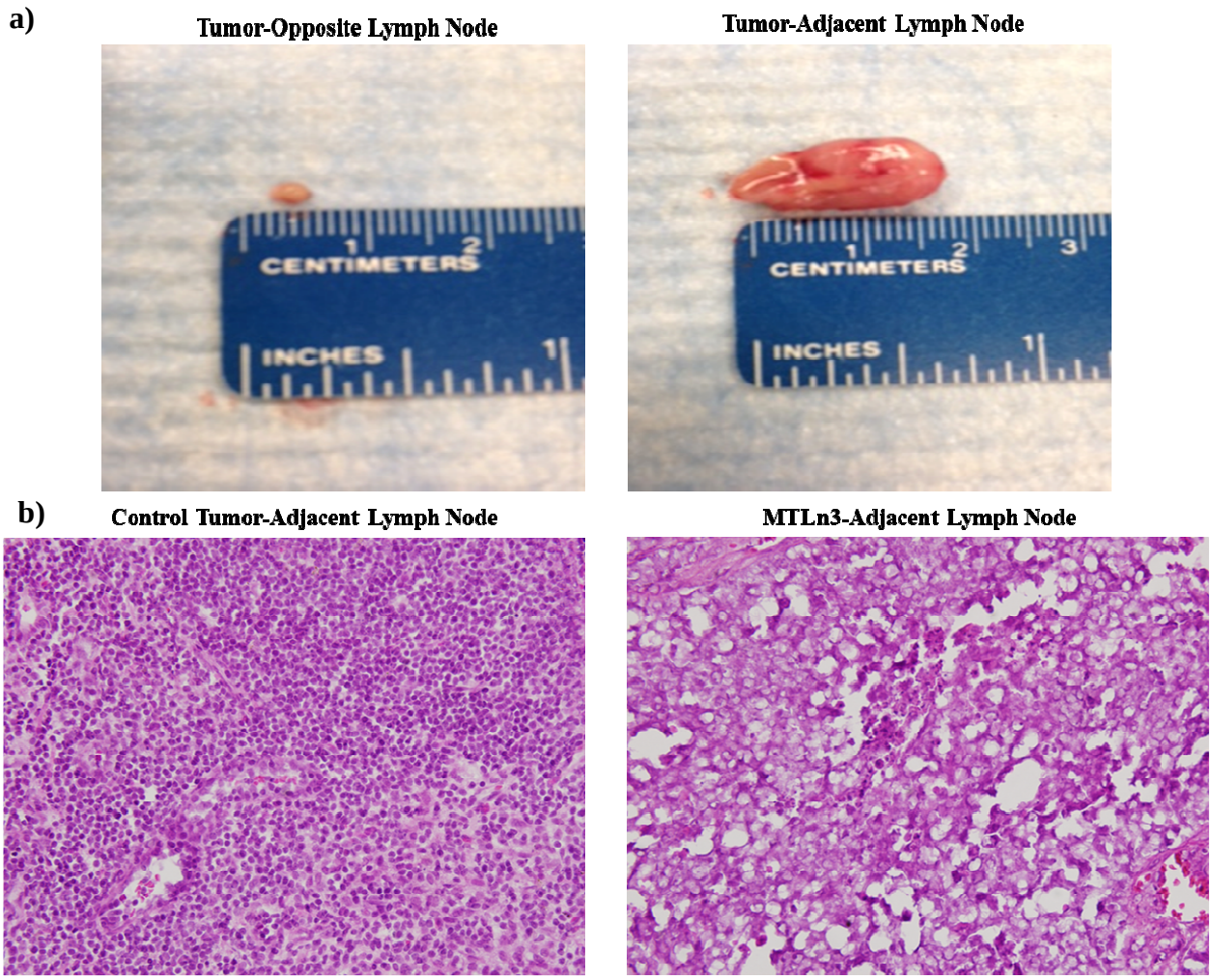

Figure 2. MTLn3 induced pathology in the tumor-adjacent lymph node. Tumor adjacent lymph nodes and tumor-opposite lymph nodes were excised 25 and 30 days post-injections. Tumor-opposite lymph node and tumor-adjacent lymph node are pictured at day 25 (a). Control and MTLn3 tumor-adjacent lymph node at day 30 were H&E stained and viewed at 40x on the fluorescent microscope (b).

Table 1. Leukocytes expanded in the spleen on day twenty-one

Spleen					
Cells x 10^6	**Day 0**	**Day 7**	**Day 14**	**Day 21**	**Day 25**
CD4+ T Cells	14.1 ± 2.90	14.0 ± 1.54	8.51 ± 0.86	97.6 ± 36.3*	14.5 ± 1.31
CD8+ T Cells	8.60 ± 1.12	7.78 ± 0.74	4.81 ± 0.51	13.8 ± 0.65*	8.54 ± 0.96
B Cells	3.27 ± 0.32	4.70 ± 0.67	3.82 ± 0.28	51.2 ± 12.6**	12.6 ± 1.57
NK Cells	3.00 ± 0.32	2.08 ± 0.25	2.09 ± 0.24	6.69 ± 1.15*	5.39 ± 0.68
Dendritic Cells	1.87 ± 0.32	2.17 ± 0.19	1.92 ± 0.27	6.48 ± 1.40**	3.81 ± 0.29
Macrophages	11.7 ± 2.71	14.9 ± 1.42	12.2 ± 1.37	40.7 ± 6.98**	13.7 ± 1.73

On day 0, rats were assigned to a control group (day 0) or injected with 1 x 10^6 MTLn3 tumor cells. On day 0, 7, 14, 21 or 25 days after injection, rats were euthanized and spleens were removed to enumerate leukocyte populations. Data are means ± SEM total leukocytes x 10^6 for spleen for 5 experiments. Statistical analysis was performed using One-Way ANOVA with Tukey post-test. * denotes $p < 0.01$, ** denotes $p < 0.001$ when compared to control group (day 0). N=8-13 rats per group.

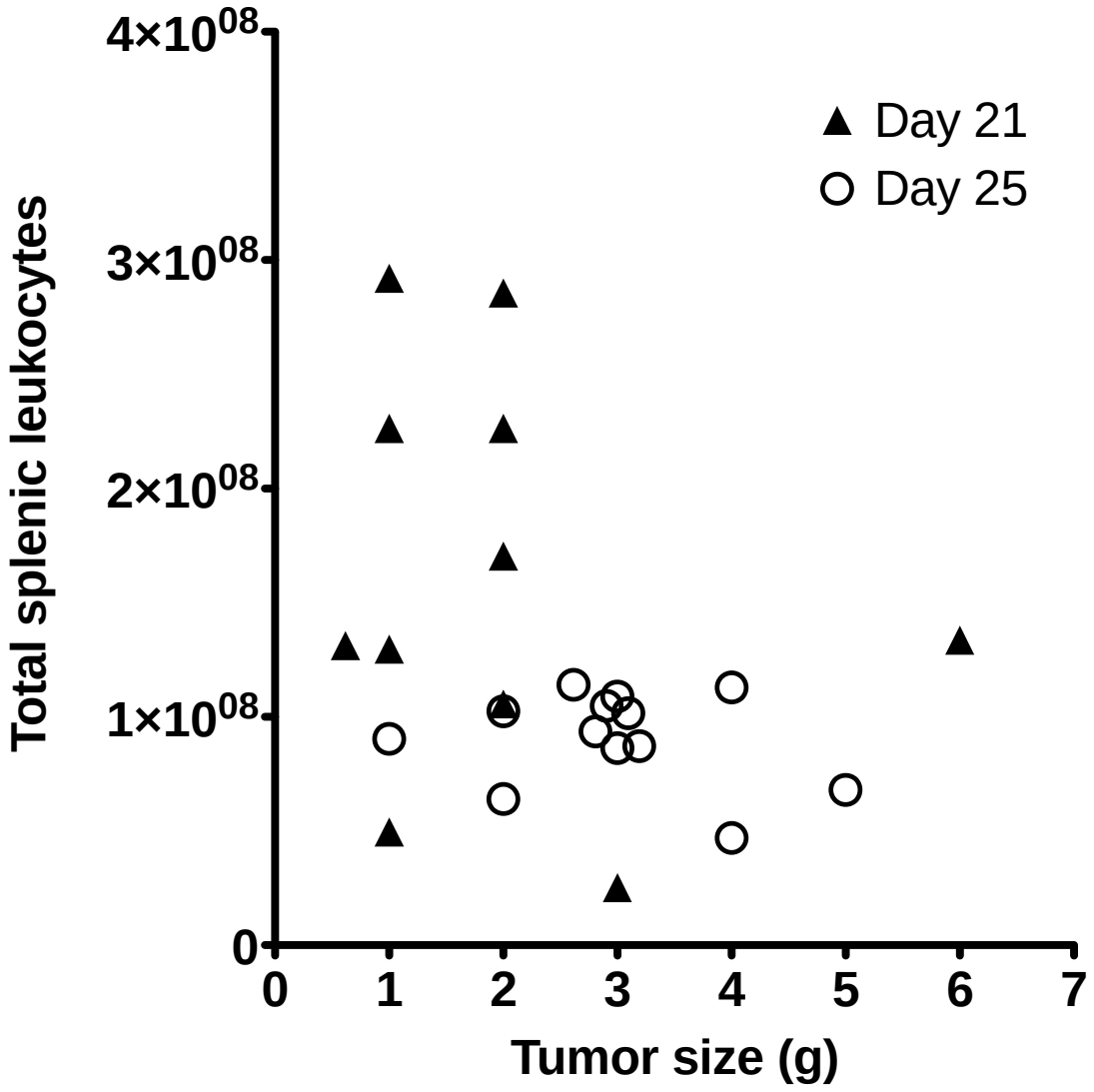

Figure 3. Splenic leukocyte concentrations do not correlate with tumor size. On day 0 rats were subcutaneously injected with $1x10^6$ MTLn3 cells/mL. On days 21 and 25, tumors and spleen were excised. Tumors were weighed *ex vivo* and total splenic leukocytes were counted with the Hemavet. Correlation analysis was performed between tumor size (in grams) and total splenic leukocytes using spearman coefficient. N=11-14.

Table 2. Leukocytes increased in the tumor-adjacent lymph node at day twenty-five

a). Tumor-Adjacent Lymph Node					
Cells x 10^5	**Day 0**	**Day 7**	**Day 14**	**Day 21**	**Day 25**
CD4+ T Cells	2.28 ± 0.64	2.40 ± 0.67	2.00 ± 0.37	2.72 ± 0.98	5.54 ± 0.90*
CD8+ T Cells	0.72 ± 0.20	1.05 ± 0.32	1.01 ± 0.22	1.83 ± 0.67	4.29 ± 0.79***
B Cells	0.66 ± 0.12	0.82 ± 0.29	1.03 ± 0.30	1.19 ± 0.50	6.48 ± 1.83**
NK Cells	0.13 ± 0.04	0.02 ± 0.00	0.34 ± 0.11	0.40 ± 0.12	1.44 ± 0.51*
Dendritic Cells	0.96 ± 0.23	0.79 ± 0.16	1.39 ± 0.29	1.69 ± 0.73	4.90 ± 1.28*
Macrophages	0.55 ± 0.11	0.42 ± 0.11	0.85 ± 0.26	0.80 ± 0.25	20.13 ± 6.07**

b). Tumor-Opposite Lymph Node					
Cells x 10^5	**Day 0**	**Day 7**	**Day 14**	**Day 21**	**Day 25**
CD4+ T Cells	2.40 ± 0.48	2.36 ± 0.47	1.56 ± 0.25	2.83 ± 1.72	1.70 ± 0.43
CD8+ T Cells	1.04 ± 0.18	0.91 ± 0.17	0.68 ± 0.11	1.21 ± 0.69	0.86 ± 0.21
B Cells	1.23 ± 0.43	0.91 ± 0.33	0.73 ± 0.21	0.74 ± 0.28	0.41 ± 0.06
NK Cells	0.14 ± 0.05	0.02 ± 0.00	0.21 ± 0.06	0.25 ± 0.08	0.63 ± 0.18*
Dendritic Cells	1.67 ± 0.37	1.37 ± 0.36	1.30 ± 0.34	1.50 ± 1.14	1.13 ± 0.29
Macrophages	0.63 ± 0.09	0.55 ± 0.09	0.56 ± 0.08	0.67 ± 0.16	2.09 ± 0.61

On day 0, rats were assigned to a control group (day 0) or injected with 1 x 10^6 MTLn3 tumor cells. On day 0, 7, 14, 21 or 25 days after injection, rats were euthanized and tumor-adjacent lymph nodes and tumor-opposite lymph nodes were removed to enumerate leukocyte populations. Data are means ± SEM total leukocytes x 10^5 for lymph nodes for 5 experiments. Statistical analysis was performed using One-Way ANOVA with Tukey post-test. * denotes $p < 0.05$, ** denotes $p < 0.01$, and *** denotes $p < 0.001$ when compared to control group (day 0). N=8-13 rats per group.

Table 3. Leukocytes migrated into the lung between days fourteen to twenty-five

Lung					
Cells x 10^5	**Day 0**	**Day 7**	**Day 14**	**Day 21**	**Day 25**
CD4+ T Cells	0.26 ± 0.06	0.24 ± 0.06	0.07 ± 0.00	0.37 ± 0.07	0.10 ± 0.03
CD8+ T Cells	0.12 ± 0.02	0.14 ± 0.04	0.04 ± 0.00	0.16 ± 0.03	0.04 ± 0.01
B Cells	2.62 ± 0.46	2.87 ± 0.40	3.16 ± 0.47	2.08 ± 0.15	1.03 ± 0.31*
NK Cells	0.16 ± 0.04	0.23 ± 0.03	0.18 ± 0.03	1.15 ± 0.31**	0.53 ± 0.20
Dendritic Cells	0.31 ± 0.08	0.27 ± 0.03	0.59 ± 0.08**	0.16 ± 0.02	0.17 ± 0.03
Macrophages	2.43 ± 0.31	2.78 ± 0.37	2.27 ± 0.26	1.87 ± 0.17	1.60 ± 0.30

On day 0, rats were assigned to a control group (day 0) or injected with 1 x 10^6 MTLn3 tumor cells. On day 0, 7, 14, 21 or 25 days after injection, rats were euthanized and lungs were removed to enumerate leukocyte populations. Data are means ± SEM total leukocytes x 10^5 for lung for 5 experiments. Statistical analysis was performed using One-Way ANOVA with Tukey post-test. * denotes $p < 0.05$ and ** denotes $p < 0.01$ when compared to control group (day 0). N=9 rats per group.

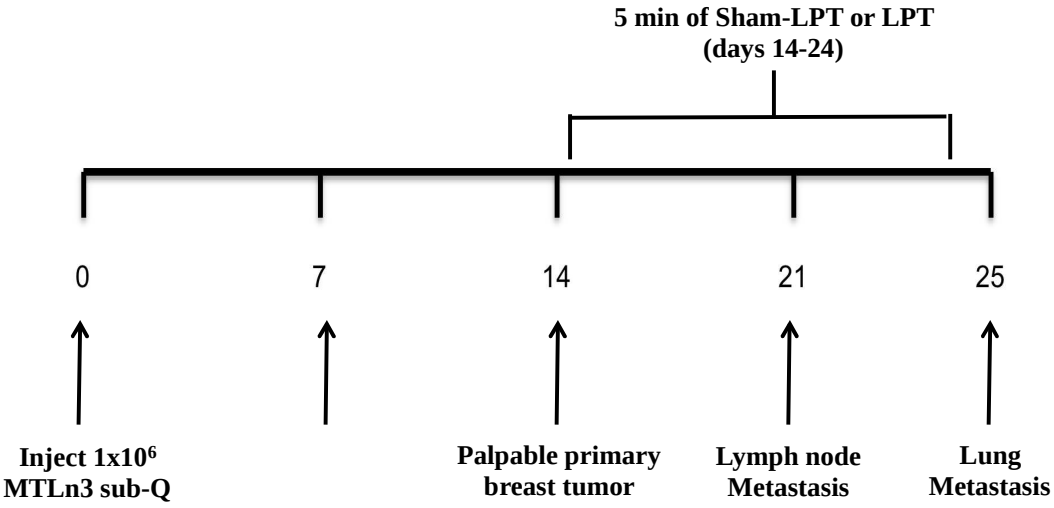

Figure 4. Study design timeline. Rats were assigned to control (Day 0) group or were subcuataneously injected with $1x10^6$ MTLn3 cells/mL (MTLn3). Rats were euthanized 0, 7, 14, 21 or 25 days post-injection. Some rats were also divided into treatment groups: MTLn3+Sham-LPT or MTLn3+LPT and treated for nine days between days 14-24 as previously described. Rat that received treatment were euthanized on day 25. Lungs, tumor-adjacent lymph nodes, tumor-opposite lymph nodes, spleens and primary tumors were excised. Cardiac puncture was also performed.

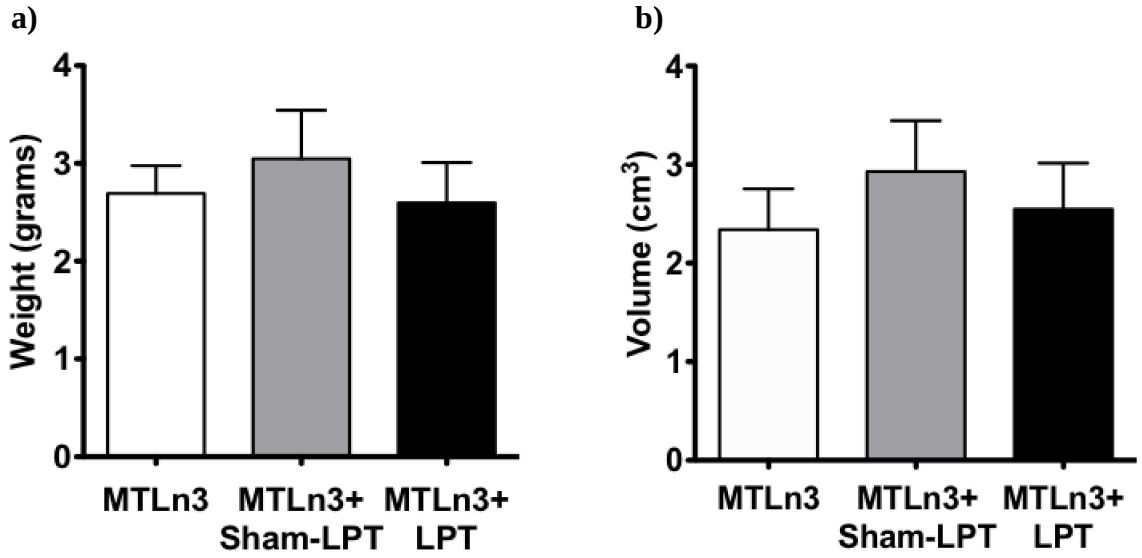

Figure 5. LPT did not enhance primary tumor growth. On day 0, rats were subcutaneously injected with 1 x 10^6 MTLn3 tumor cells and divided into MTLn3, MTLn3+Sham-LPT or MTLn3+LPT and received treatment for nine days as previously described. On day 25, rats were euthanized and primary tumors were collected. Tumor weights were measured *ex vivo.* Tumor volume was measured *in situ* with calipers and volume was calculated using the equation: (L x W^2) x (π/6). Data are means ± SEM weight in grams (a) and volume in cm^3 (b) for 3 experiments. Statistical analysis was performed using One-Way repeated measures ANOVA with Tukey post-test. N=19 rats per group.

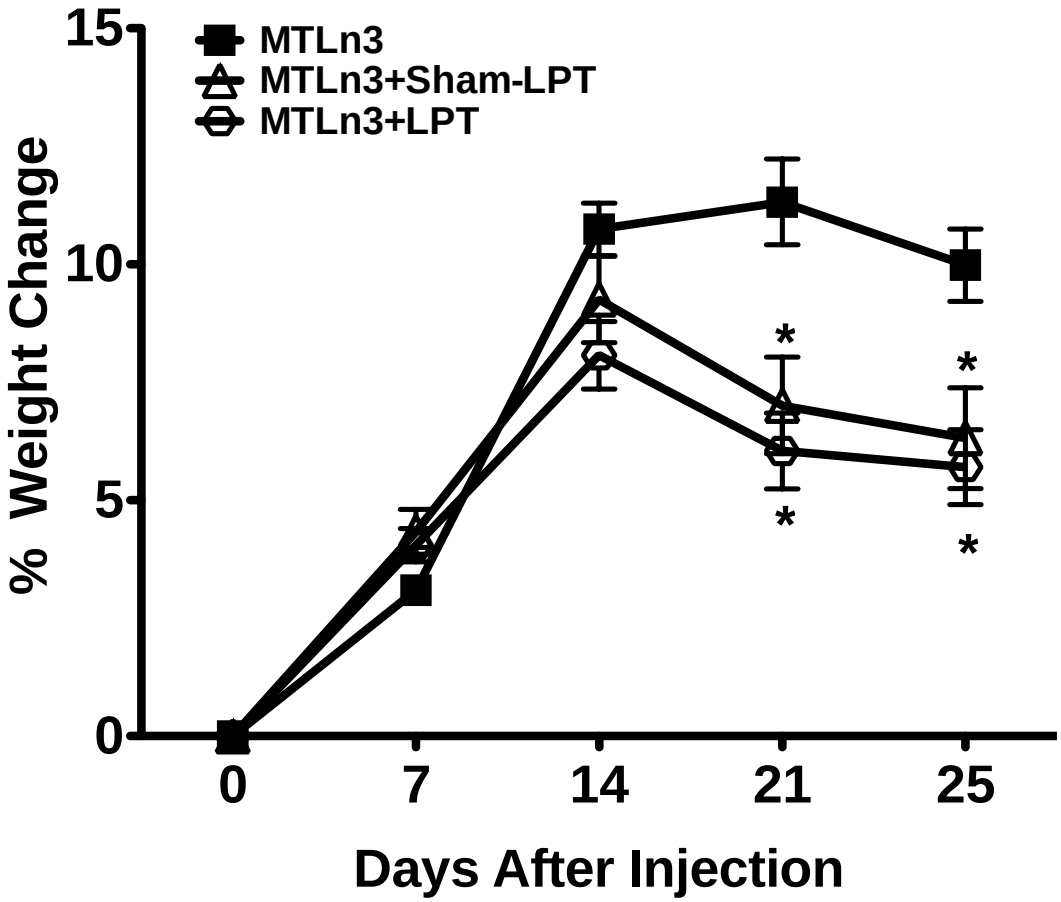

Figure 6. Sham and LPT cause weight loss. On day 0, rats were subcutaneously injected with 1 x 10^6 MTLn3 tumor cells and divided into control, MTLn3, MTLn3+Sham-LPT or MTLn3+LPT and received treatment for nine days as previously described. Rats were weighed weekly for 25 days. Data are means ± SEM percent weights for 3 experiments. Statistical analysis was performed using Two-Way repeated measures ANOVA with Tukey post-test. * denotes $p < 0.0001$ when compared to MTLn3. N = 18 rats per group.

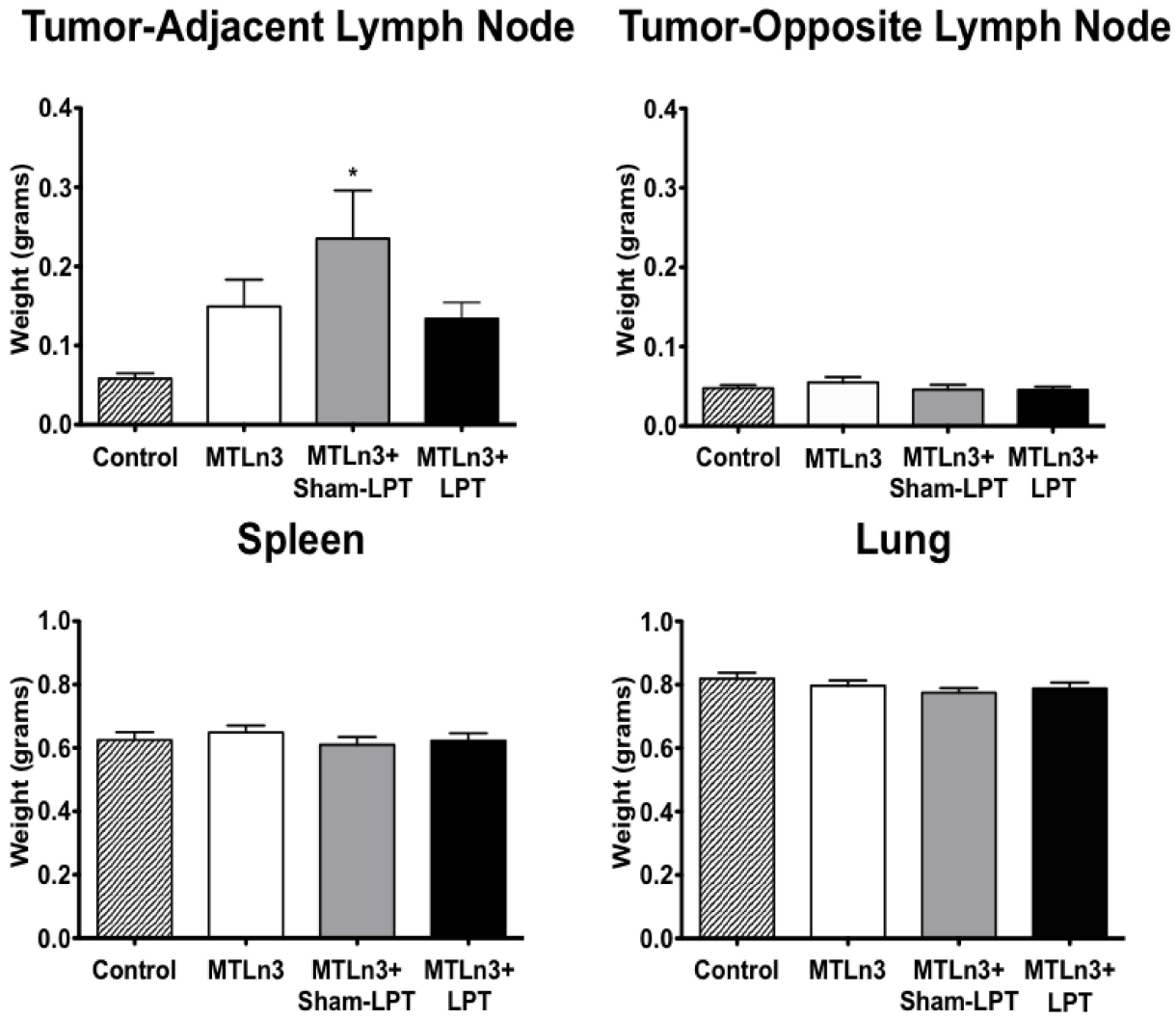

Figure 7. LPT protects against pathogenesis induced by anesthesia in tumor-adjacent lymph node. On day 0, rats were subcutaneously injected with 1 x 10^6 MTLn3 tumor cells and divided into control, MTLn3, MTLn3+Sham-LPT or MTLn3+LPT group and received treatment for nine days as previously described. On day 25, rats were euthanized and ALN, OLN, lung and spleens were excised and weighed. Data are means ± SEM weight in grams for 3 experiments. Statistical analysis was performed using One-Way ANOVA with Tukey post-test. * denotes $p < 0.05$ when compared to healthy group. N=7-12 rats per group.

Table 4. Sham and LPT inhibited leukocytosis during MTLn3 disease

10^6 cells/mL	Control	MTLn3	MTLn3+ Sham-LPT	MTLn3+ LPT
Total WBC's	1.87 ± 0.18	2.91 ± 0.14***	1.69 ± 0.08	1.78 ± 0.11
Neutrophils	0.42 ± 0.04	1.01 ± 0.08**	0.54 ± 0.03	0.59 ± 0.06
Lymphocytes	1.35 ± 0.16	1.75 ± 0.08*	1.07 ± 0.07	1.09 ± 0.07
Monocytes	0.08 ± 0.00	0.14 ± 0.01*	0.08 ± 0.00	0.09 ± 0.01

On day 0, rats were subcutaneously injected with 1 x 10^6 MTLn3 tumor cells and divided into control, MTLn3, MTLn3+Sham-LPT or MTLn3+LPT group and received treatment for nine days as previously described. Cardiac puncture was performed 25 days post-injection and blood was analyzed on Hemavet. Data are means ± SEM number of cells (x10^6 cells/mL) for 3 experiments. Statistical analysis was performed using One-Way ANOVA with Tukey post-test. * denotes $p < 0.05$, ** denotes $p < 0.01$, and *** denotes $p < 0.001$. N=12-18 rats per group.

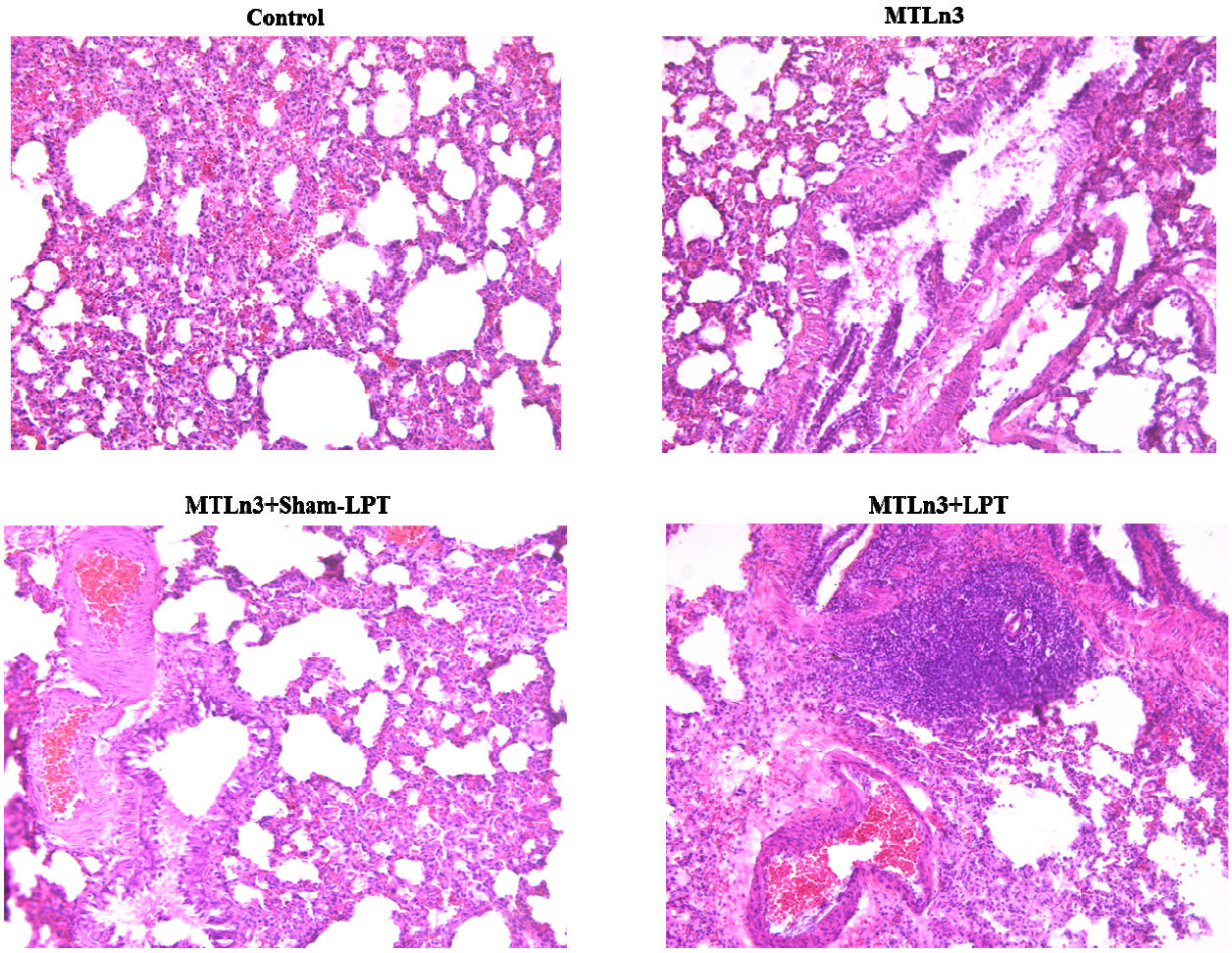

Figure 8. Sham and LPT induce pathology in the lung during MTLn3 disease. Lungs from all groups were removed at day 25 post-injection. Tissues were stained with hematoxylin and eosin. Images are of the left lung lobe at 20X magnification.

REFERENCES

1. Neri A, Welch D, Kawaguchi T, Nicolson GL. Development and biologic properties of malignant cell sublines and clones of a spontaneously metastasizing rat mammary adenocarcinoma. *JNatl Cancer Inst.* 1982;68(3):507–517.

2. Welch DR, Neri A, Nicolson GL. Comparison of 'spontaneous' and 'experimental' metastasis using rat 13762 mammary adenocarcinoma metastatic cell clones. *Invasion Metastasis.* 1983;3(2):65–80.

3. J. van Nimwegen M, Verkoeijen S, Kuppen P J.K., Velthuis J H. L., van de Water B. An improved method to study NK-independent mechanisms of MTLN3 breast cancer lung metastasis. *Clin Exp Metastasis.* 2007;24:379–387.

4. Lai H, Nakase I, Lacoste E,. Singh N.P., Sasaki T. Artemisinin-transferrin conjugate retards growth of breast tumors in the rat. *Anticancer Research.* 2009;29:3807-3810.

5. Youlden DR, Cramb SM, Dunn NAM, Muller JM, Pyke CM, Baade PD. The descriptive epidemiology of female breast cancer: An international comparison of screening, incidence, survival and mortality. *Cancer Epidemiology.* 2012;36:237-248.

6. Eickmeyer SM, Gamble GL, Shahpar S, Do KD. The Role and efficacy of exercise in persons with cancer. *PM R.* 2012;4:874-881.

7. Curigliano Giuseppe. Immunity and autoimmunity: revising the concepts of response to breast cancer. *The Breast.* 2011;20:S71-S74.

8. Vivier E, Raulet DH, Moretta A, et al. Innate or adaptive immunity? The example of natural killer cells. *Science.* 2011;331:44-49.

9. Dranoff G. Cytokines in cancer pathogenesis and cancer therapy. *Nat Rev Cancer*. 2004;4(1):11-22.

10. Melvold RW, Sticca RP. Basic and tumor immunology: a review. *Surg Oncol Clin N Am*. 2007;16(4):711-35, vii.

11. Yanofsky V, Mitsui H, Felsen D, Carucci J. Understanding dendritic cells and their role in cutaneous carcinoma and cancer immunotherapy. *Clin & Dev Imm.* 2013;2013:1-14.

12. Roberti MP, Mordoh J, Levy EM. Biological role of NK cells and immunotherapeutic approaches in breast cancer. *FIMMU.* 2012;3(175):1-11.

13. Murphy K, Travers P, Walport M. *Janeway's Immunobiology*, (8th Ed), Garland Science, New York, 2012.

14. Blumencranz PW, Piereti M, Allen KG, Blumencranz LE. Molecular analysis of breast sentinel lymph nodes. *Surg Oncol Clin N Am.* 2011;20:467-485.

15. Francissen C.M.T.P., Dings PJM, van Dalen T, Strobbe LJA, van Laarhoven HWM, de Wilt JHW. Axillary recurrence after a tumor-positive sentinel lymph node biopsy without axillary treatment: a review of the Literature. *Ann Surg Oncol.* 2012;19:4140–4149.

16. Hodge LM, Downey FH. Lymphatic pump treatment enhances the lymphatic and immune systems. *Exp Biol Med.* 2011;236:1109-1115.

17. Sakorafasa GH, Perosa G, Cataliottib L, Vlastosc G. Lymphedema following axillary lymph node dissection for breast cancer. *Surg Onco.* 2006;15:153–165.

18. Moseley AL, Carati CJ, Piller NB. A systematic review of common conservative therapies for arm lymphoedema secondary to breast cancer treatment. *Annals of Oncology.* 2007;18: 639–646.

19. Stacker SA, Baldwin ME, Achen MG. The role of tumor lymphangiogenesis in metastatic spread. *FASEB J.* 2002;16(9): 922-34.

20. Knott EM, Tune JD, Stoll ST, Downey HF. Increased lymphatic flow in the thoracic duct during manipulative intervention. *J Am Osteopath Assoc.* 2005;105(10):447-56.

21. Ran S, Volk L, Flister M. Lymphangiogenesis and lymphatic metastasis in breast cancer. *Pathophys.* 2010;17:229-251.

22. Olszewski WL. The lymphatic system in body homeostasis: physiological conditions. *Lymphat Res Biol.* 2003;1:11–21.

23. Hodge LM, Bearden MK, Schander A, Huff JB, Williams Jr. A, King HH, Downey FH. Lymphatic pump treatment mobilizes leukocytes from the gut associated lymphoid tissue into lymph. *Lymphat Res Biol.* 2010;8(2):103-110.

24. Chiang A, Massague J. Molecular basis of metastasis. *N Engl J Med.* 2008;359(26):2814-

25. Bacurau AVN, Belmonte MA, Navarro F, Moraes MR, Pontes Jr FL, Pesquero JL, Araujo RC, Bacurau RFP. Effect of a high-intensity exercise training on the metabolism and function of macrophages and lymphocytes of walker 256 tumor-bearing rats. *Exp Biol Med.* 2007;232:1289-99.

26. Huff JB, Schander A, Downey HF, Hodge LM. Lymphatic pump treatment augments lymphatic flux of lymphocytes in rats. *Lymphat Res Biol.* 2010;8(4):183-87.

27. Schander A, Downey FH, Hodge LM. Lymphatic pump manipulation mobilizes inflammatory mediators into lymphatic circulation. *Exp Biol Med.* 2011;237:58-63.

28. Nagata H, Arai T, Soejima Y, et al. Limited capability of regional lymph nodes to eradicate metastatic cancer cells. *Cancer Res.* 2004; 64:8239-8248.

29. Brown JC, Cheville AL, Tchou JC, Harris SR and Schmitz KH. Prescription and adherence to lymphedema self-care modalities among women with breast cancer-related lymphedema. *Support Care Cancer*. 2013; 22(1):135-43.

30. Lesho EP. An overview of osteopathic medicine. *Arch Fam Med.* 1999;8(6): 477-84.

31. Hutnick NA, Williams NI, Kraemer WJ, Orsega-Smith E, Dixon RH, Bleznak AD, Mastro AM. Exercise and lymphocyte activation following chemotherapy for breast cancer. *Med Sci Sports Exerc.* 2005;37(11):1827-35.

32. Hayes et al. Lymphedema after breast cancer: Incidence, risk factors, and effect on upper body function. *J Clin Oncol.* 2008;26:3536-3542.

33. Cowin P and Welch D. Breast cancer progression: Controversies and consensus in the molecular mechanisms of metastasis and EMT. *J Mammary Gland Biol Neoplasia.* 2007;12: 99–102.

34. Degenhardt BF, Kuchera ML. Update on osteopathic medical concepts and the lymphatic system. *J Am Osteopath Assoc.* 1996;96(2):97-100.

35. Noll DR, Degenhardt BF, Morely TF, Blais FX, Hortos KA, Hensel K, Johnson JC, Pasta DJ, Stoll T. Efficacy of osteopathic manipulation as an adjunctive therapy for hospitalized patients with pneumonia: a randomized controlled trial. *Osteopath Med Prim Care.* 2010;4:2.

36. Crowe JP Jr, Gordon NH, Shenk RR, Zollinger RM Jr, Brumberg DJ, Shuck JM. Primary tumor size. Relevance to breast cancer survival. *Arch Surg.* 1992;127(8):910-5.

37. Miyata T, Kodama T, Honma R, Nezu Y, Harada Y, Yogo T, Hara Y, Tagawa M. Influence of general anesthesia with isoflurane following propofol-induciton on natural killer cell cytotoxic activities of peripheral blood lymphocytes in dogs. *J Vet Med Sci.* 2013;75(7):917-21.

38. Rowe RW, Tomoda M, Strebel FR, Jenkins GN, Stephens LC, Bull JMC. The natural progression of microvasculature in primary tumor and lymph node metastases in a breast carcinoma model. *Cancer Biol Ther.* 2004;3(4):408-14.

39. McCauley L, Pedrueza M, Zhang X, Jones H, Hodge LM. Lymphatic pump treatment

enhances pulmonary immunity and protects against solid tumor formation in the rat lung. *AAI abstract.* 2011.

40. Hodge LM. Osteopathic lymphatic pump techniques to enhance immunity and treat pneumonia. *Int J Osteopath Med.* 2012;15(1):13-21.

41. Creasy C, Schander A, Orlowski A, Hodge LM. Thoracic and abdominal lymphatic pump techniques inhibit the growth of S. pneumoniae bacteria in the lungs of rats. *Lymphat Res Biol*. 2013;11(3);183-6.

42. Allen TW, Pence TK. The use of the thoracic pump in treatment of lower respiratory tract disease. *J Am Osteopath Assoc.* 1967;67:408-411.

43. Takeno Y, Arita H, Fujimoto E. Efficacy of complete decongestive therapy (CDT) on edematous rat limb after lymphadenectomy demonstrated by real time lymphatic fluid tracing. *SpringerPlus.* 2013;2:225.

44. Janeway CA Jr, Travers P, Walport M, et al. Immunobiology: The immune system in health and disease. 5th ed. New York; Garland Science; 2001. The mucosal immune system.

45. Acheson D, Luccioli S. Mucosal immune responses. *Best Practice and Research Clinical Gastroenterology.* 2004;18(2):387-404.